

DANIELE PEANO (*), MARTA CHIARLE (**) & JOST VON HARDENBERG (***)

A MINIMAL MODEL APPROACH FOR GLACIER LENGTH MODELING IN THE WESTERN ITALIAN ALPS

ABSTRACT: PEANO D., CHIARLE M. & VON HARDENBERG J., *A minimal model approach for glacier length modeling in the Western Italian Alps*. (IT ISSN 0391-9838, 2016)

We study the response of a set of glaciers in the Western Italian Alps to climate variations using a minimal glacier modeling approach, first introduced by Oerlemans. The mathematical models are forced over the period 1959-2009, using temperature and precipitation recorded by a dense network of meteorological stations, and we find a good match between the observed and modeled glacier length dynamics, especially for the two glaciers that have observed surface mass balance, i.e. Ciardoney and Grand Etrèt, and, in absence of observed surface mass balance, for small glaciers, such as Basei, Bessanese, and Capra. Forcing the model with future projections from a state-of-the-art global climate model in the RCP 4.5 and RCP 8.5 scenarios, we show how this approach can be used to obtain a first estimate for the future evolution of these glaciers length and we discuss the related uncertainties.

KEY WORDS: Minimal glacier model, Western Italian Alps, Surface mass balance, Glaciers length reconstruction.

RIASSUNTO: PEANO D., CHIARLE M. & VON HARDENBERG J., *Un approccio con un modello minimale per la modellazione della lunghezza dei ghiacciai nelle Alpi Occidentali Italiane* (IT ISSN 0391-9838, 2016)

È stata studiata la risposta di un gruppo di ghiacciai delle Alpi Italiane Occidentali alle variazioni climatiche per mezzo di un modello

(*) IRPI-CNR, Torino, Italy, now at Ca' Foscari University, Venice, Italy and CMCC, Bologna, Italy

(**) IRPI-CNR, Torino, Italy

(***) ISAC-CNR, Torino, Italy

Corresponding author: daniele.peano@cmcc.it

We thank L. Mercalli and D. Cat Berro of SMI for the Ciardoney data, S. Cerise and V. Bertoglio of GPNP for the Grand Etrèt data and S. Bertotto for providing the initial geometric data of the glaciers. We are grateful to the voluntary personnel of the Italian Glaciological Committee for monitoring glacier snout fluctuations. Without the dedicated efforts of all these field observers and scientists, studies like this one could not be performed. This work has been supported by the Project of Interest NextData of the Italian Ministry of University, Education and Research (MIUR).

minimale, introdotto per primo da Oerlemans. Questo modello matematico è stato forzato sul periodo 1959-2009, usando temperature e precipitazioni registrate da un'ampia rete di stazioni meteorologiche. Questa operazione ha permesso di trovare un buon riscontro tra la dinamica delle variazioni in lunghezza dei ghiacciai modellata e quella documentata dagli operatori glaciologici. Tale riscontro è particolarmente buono per i due ghiacciai per i quali si dispongono di misure di bilancio di massa superficiale, i.e. Ciardoney e Grand Etrèt, e, in assenza di dati di bilancio di massa, per ghiacciai di piccole dimensioni, quali Basei, Bessanese e Capra. Forzando il modello con proiezioni future simulate da un modello di clima globale allo stato-dell'arte sotto gli scenari RCP 4.5 e RCP 8.5, è stato mostrato come questo approccio possa essere usato per ottenere una prima stima dell'evoluzione futura della lunghezza di questi ghiacciai, e ne sono state discusse le incertezze.

TERMINI CHIAVE: Modello minimale di ghiacciai, Alpi Italiane Occidentali, Bilancio di massa superficiale, Ricostruzione della lunghezza dei ghiacciai.

INTRODUCTION

Climatic variations in mountain areas can lead to important environmental hazards such as landslides and floods (e.g. Deline & *alii*, 2012; Chiarle & Mortara, 2008; Stoffel & Huggel, 2012) or to changes in water availability and quality (e.g. Braun & *alii*, 2000; Viviroli & *alii*, 2011; Beniston, 2012). Mountain environments may respond strongly to climate change and different aspects of mountain regions respond to ongoing climate fluctuations; for example, the surface air temperature increase in the 20th century in the Alps has been twice the global average (Brunetti & *alii*, 2006). Alpine glaciers may present a strong and rapid reaction to climate oscillations (e.g. Nesje & Dahl, 2000; Bonanno & *alii*, 2013).

The Alpine region is characterized by an abundance of glaciers (Zemp & *alii*, 2008), but only a few of them are well studied. Time series of frontal variations are the most frequently available data. The response of glaciers to climate forcing is determined both by their geometry and

by the climatic setting and accordingly some glaciers are more sensitive to variations of winter precipitation, while others are more sensitive to summer temperatures (e.g. Letréguilly, 1988; Vincent & alii, 2005).

Different models have been developed to understand and study the evolution of glaciers, starting from measured time series, ranging from linear and zero dimensional models, such as the “minimal model” presented by Oerlemans (2011), to one or higher dimensional models, such as flowline model and full thermo-mechanical models (e.g. Oerlemans, 1997; Pattyn, 2002; Zwinger & alii, 2007). More complex models can be difficult to use for a large number of glaciers, and in fact have been rarely used in the literature, due to the large number of detailed information on each glacier which they may require and to the “under sampling problem” that imposes strong limitations on the number of model parameters and on their reliability (Marzeion & alii, 2012). As a consequence, direct modeling is often avoided and simple models or extrapolations are used (e.g. Raper & Braithwaite, 2006; Meier & alii, 2007). Simple models present the advantage that they require only few input data and so they can be used to perform estimates of the sensitivity of a high number of glaciers to changes in climate parameters. When forced with future climate scenario data, they can provide a first picture of the possible future evolution of the glaciers.

In this work we demonstrate the application and the usefulness of extremely simple models for the study of a set of glaciers in the Western Italian Alps, for which only limited information is available, by adapting and testing versions of the minimal glacier model developed by Oerlemans (2011).

AVAILABLE DATA

Study area

We focus on the Western Italian Alps, which host more than 40% of the total glacierized area of the Italian Alps, with some of the largest Italian glaciers (Smiraglia & alii, 2015; Salvatore & alii, 2015).

The locations of the glaciers considered in this work are shown in figure 1. These glaciers have been selected based on the availability and quality of glaciological data, and they represent glaciers with different characteristics in terms of size, shape, bed slope and exposition.

The Ciardoney and Grand Etrèt Glaciers (Gran Paradiso Massif) have the longest and most complete series of mass balance measurements that allow a mathematical model to be forced directly with the measured mass gain data. Nine additional glaciers, for which surface mass balance information is not available (Basei, Bessanese, Capra, Lys, Moncorvè, Mulinet Nord, Mulinet Sud, Prè de Bar and Valtournanche), are modeled assuming an empirical relationship between mass gain and climate variables. These latter glaciers were selected because a reliable time series of length fluctuation data was available for each of them. The main properties of the glaciers considered here are listed in table 1 and in Appendix A.

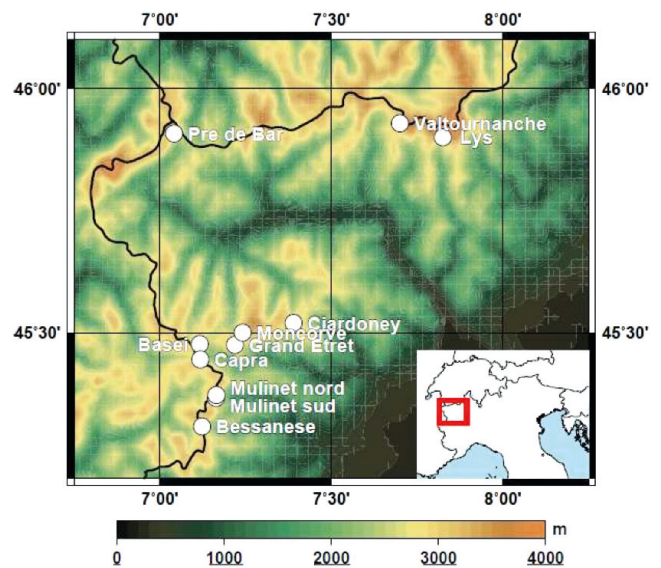


FIG. 1 - Locations of the eleven glaciers studied in this work.

Glaciological data

We use glacier length measurements provided by the Italian Glaciological Committee, which has collected and published measurements for these glaciers since the beginning of the last century (<http://www.glaciologia.it/>). Annual surface mass gain and Equilibrium Line Altitude (ELA) measurements for the Ciardoney Glacier have been collected by the Italian Meteorological Society (SMI; <http://www.nimbus.it>). The surface mass balance of the Grand Etrèt Glacier has been measured by the personnel of the Gran Paradiso National Park (GNP; <http://www.pnnp.it/>). In particular, for the Ciardoney Glacier length measurements for the period 1971-2009 and mass balance measurements for the period 1992-2000 are available (fig. 2a); for the Grand Etrèt Glacier length measurements for the period 1997-2009 and mass balance measurements for the period 2000-2009 are available (fig. 2b).

Values of geometrical parameters, such as reference length, glacier minimum and maximum height, have been obtained in a Geographic Information System (GIS) environment from aerial images released by the Italian Ministry of Environment, taken during flights in 2000 and 2006 (<http://www.pcn.minambiente.it/GN>), and are summarized in table 1 and in Appendix A.

Climate data

Temperature and precipitation, recorded by a dense network of meteorological stations, are made available by the Regional Agency for Environmental Protection of Piedmont, Italy (ARPA; <http://www.arpa.piemonte.it>). In this work we use seasonal averages derived from daily values, regridded onto a regular grid ($0.125^\circ \times 0.125^\circ$, almost 14 km) using an Optimal Interpolation (OI) technique (Uboldi & alii, 2008), for the Piemonte and Valle d'Aosta regions in Northwestern Italy during the period

TABLE 1 - Values of the geometrical parameters used to describe the geometry of the studied glaciers. The initial year of the series of measured values and the number of measured years are reported in the second and third columns respectively. L_{yrI} represents the glacier length at the initial year, these values have been obtained by adding the field measured length oscillations to the glacier length acquired in a GIS environment using the 2000 or 2006 aerial photos; b_0 is the elevation of the glacier's head; s is the estimated mean slope of the glacier's bed. The values of L_{yrI} , b_0 and s have been measured using GIS tools

Glacier	First year	# years	L_{yrI} [m]	b_0 [m a.s.l.]	s	Mean aspect
Ciardoney	1971	28	1660	3150	0.14	E
Grand Etrèt	1997	12	1310	3100	0.29	NW
Basei	1968	27	727	3300	0.48	N-NE
Bessanese	1973	22	1866	3220	0.34	E-SE
Capra	1959	20	942	2790	0.33	N-NE
Lys	1977	33	5169	4350	0.34	SW
Moncorvè	1986	20	1603	3640	0.50	W
Mulinet Nord	1989	17	432	2980	0.50	E-SE
Mulinet Sud	1989	16	762	3000	0.39	E
Prè de Bar	1959	49	3342	3700	0.43	SE
Valtournanche	1969	27	1600	3590	0.38	W

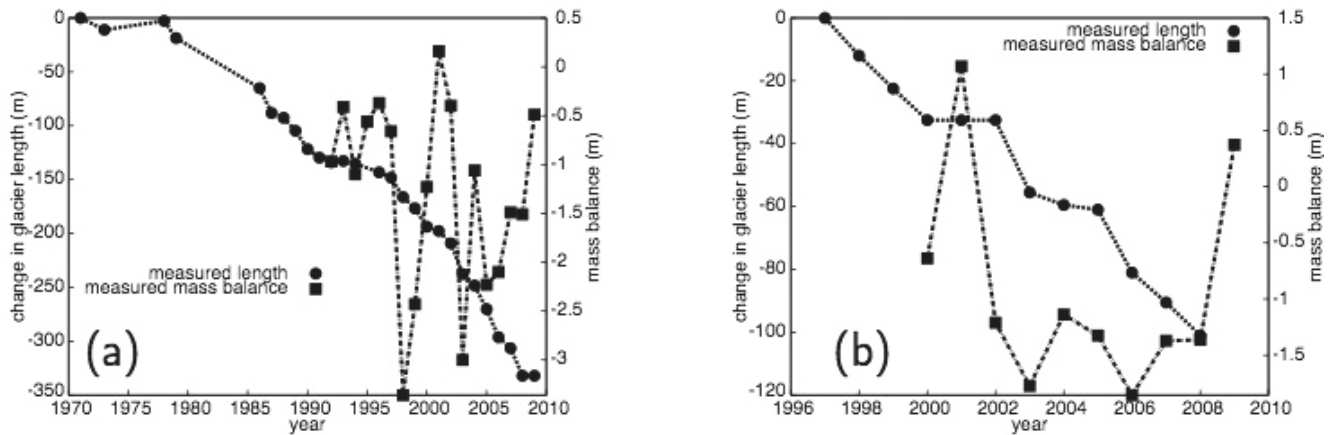


FIG. 2 - (a) Measured changes in glacier length (m , black circle) in the period 1971-2009 and mass balance (mve , black squares) in the period 1992-2009, data from SMI, for the Ciardoney Glacier. (b) Measured changes in glacier length (m , black circle) in the period 1997-2009 and mass balance (mve , black squares) in the period 2000-2009, data from GPNP for the Grand Etrèt Glacier. Note that the lines are drawn to guide the eye.

1959-2009. In the analysis, we consider seasonal averages of precipitation during the accumulation period (from October to May) and temperature during the ablation season (from June to September), in order to relate the meteorological variables to the annual surface mass balance values. We indicate these two seasonal averages as “October-May precipitation”, and “June-September temperature” respectively: the timing of these seasonal averages is taken starting from the study by Bonanno & alii (2013). The seasonal averages have been standardized by removing, for each grid point, the climatological mean in the period 1971-2000 and by dividing the standard deviation in the same period. This operation helps to better highlight the relative importance of temperature and

precipitation fluctuations in determining the mass balance variations in our approach.

Precipitation and surface temperature data from the EC-Earth Global Climate Model (GCM) over the period 1959-2100 were used to force the models to generate future projections. EC-Earth (Hazeleger & alii, 2012) is a state-of-the-art global climate model developed by a European consortium, which includes the Integrated Forecast System atmospheric model by the European Centre for Medium-range Weather Forecast (ECMWF), for the atmosphere, the Nucleus for European Modeling of the Ocean (NEMO), for the ocean component, and the land-surface module H-Tessel and the Louvain-la-neuve sea-Ice Model (LIM). The scenarios used here are

Representative Concentration Pathway (RCP) projection RCP 4.5 and RCP 8.5 (Moss & alii, 2010) prepared with EC-Earth v2.3 for the Climate Model Intercomparison Project (CMIP5) archives, using the model with atmospheric resolution 1.125° and 62 levels. These data are publicly available from the CMIP5 Earth Science Grid Federation distribution nodes (<http://cmip-pcmdi.llnl.gov/cmip5/>).

An ensemble of seven different realizations of monthly averaged values was available for the RCP 4.5 scenario and an ensemble of eight realizations was used for the RCP 8.5 scenario. All ensemble members used the same forcing but started from different initial conditions at the beginning of the historical period (in 1850).

MINIMAL GLACIER MODELS

Minimal glacier models assume a simplified glacial geometry and the time-evolution of glacier length is computed from a continuity equation for the whole glacier, typically using an instantaneous relationship between glacier length and depth. As such, they cannot describe the propagation of kinematic waves or depth variations along the glacier. Since these models include only a few parameters, they are particularly useful for the study of the interaction between glaciers and climate when limited information on the glacier characteristics is available. In the following, we use a very simple model, introduced by Oerlemans (2001, 2011) and Oerlemans & alii (2011), which consider a glacier of uniform width, resting on a bed with constant slope, with a constant mass balance gradient along the glacier.

This idealized glacier geometry is illustrated in figures 3 and 4. Ice thickness is assumed uniform along the glacier length and set equal to a mean ice thickness, $H(t)$, which can change as a function of time t . The total glacier volume is $V(t) = W H(t) L(t)$, where $L(t)$ is the time-varying glacier length and a simple relationship between the mean ice thickness value H and the glacier length L is provided by Oerlemans (2011):

$$H = \frac{\alpha_m L^{1/2}}{1 + \nu s} \quad (1)$$

where α_m and ν are constants and s is the mean constant bed slope. The value of ν is directly taken from Oerlemans (2011), while the value of α_m is tuned (table 2), since no direct information on ice thickness is available for the studied glaciers.

The two main sources of volume change for a glacier are the surface mass balance, B_s , and, if terminating in water, a calving flux (Oerlemans, 2011). Since none of the studied glaciers terminate in lakes, we ignore the calving flux in the following.

The annual mass gain of the glacier, B_s , can be estimated according to ELA oscillations, as suggested by Oerlemans (2010, 2011). Alternatively, when measured net annual mass gains or losses at specific points on the glacier (b) are available one can use the expression to calculate the overall glacier surface mass balance.

TABLE 2 - Best values for the parameters used in Eq. (1) for Ciardoney Glacier and Grand Etrêt Glacier (Basic case), and the best values for Eq. (6) (W(x) case). For the basic case the value of ν is taken from Oerlemans (2011), while the values of α are the best values obtained after a minimization of the root mean square (RMS) difference between the measured glacier length variations and the modeled ones. For the W(x) case the values of ν and w_1 are taken from Oerlemans (2011), while w_0 and w_2 are taken from geometrical information. Again the values of α_m are the best values obtained after a minimization of the RMS

	Parameter	Ciardoney	Grand Etrêt
Basic case	ν []	10	10
	$\alpha_m \left[\text{m}^{-1/2} \right]$	7.6	11.2
	RMS [m]	10.0	4.7
W(x) case	ν []	10	10
	$\alpha_m \left[\text{m}^{-1/2} \right]$	3.9	8.5
	w_0 [m]	70	53.5
	w_1 []	3	3
	$w_2 \left[\text{m}^{-1} \right]$	0.002	0.003
	RMS [m]	11.1	4.6

The temporal variation of the total glacier volume can thus be written as

$$\begin{aligned} \frac{dV}{dt} &= \frac{d}{dt} (W H L) \\ &= HW \frac{dL}{dt} + HL \frac{dW}{dt} + WL \frac{dH}{dt} \\ &= B_s = \dot{b} W L \end{aligned} \quad (2)$$

where H is given by Eq. (1) and its time derivative is

$$\frac{dH}{dt} = \frac{\alpha_m}{2(1 + \nu s)} L^{-1/2} \frac{dL}{dt} \quad (3)$$

Assuming a uniform and constant value of W , the change of glacier length becomes

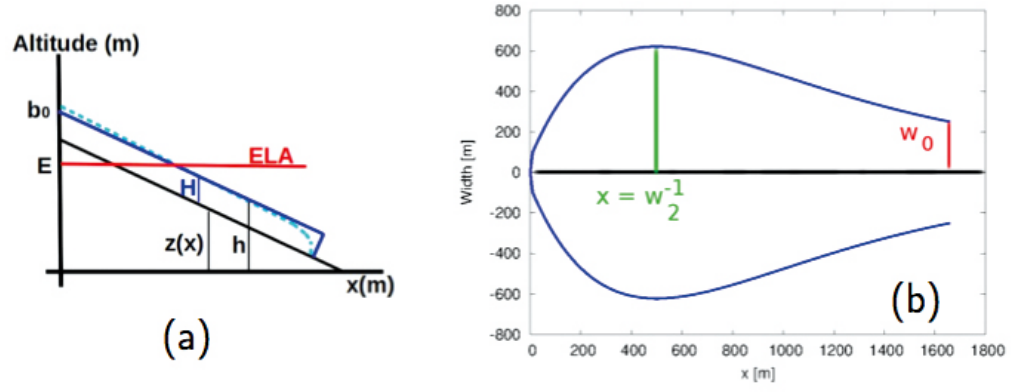
$$\frac{dL}{dt} = \frac{\dot{b} L}{\frac{3\alpha_m}{2(1 + \nu s)} L^{1/2}} \quad (4)$$

More complex geometries could also be used. For example we can consider a scaling relation between glacier length and glacier width, or a width that varies along the flow line, such as:

$$W(x) = \frac{L}{L_0} (w_0 + w_1 x e^{-w_2 x}) \quad (5)$$

where w_0 determines the width at the glacier snout and w_1 and w_2 influence the shape of the glacier: in particular, the maximum width of the glacier along the flow line is placed at $x = w_2^{-1}$ (fig. 3b; Oerlemans, 2011). We use the same relation described in Eq. (1) and Eq. (3) and we consider an average width given by $\bar{W}_m = 1/L \int_0^L W(x) dx$. In this way, we

FIG. 3 - (a) The simple glacier geometry considered in the minimal model. E represents the equilibrium line altitude, b_0 is the glacier head altitude, H represents the ice thickness, $z(x)$ is the bed altitude and $b = z(x) + H$. The dark blue line represents the geometry used here, while the light blue one represent the perfect plasticity shape. (b) The shape described in Eq. (5).



obtain a final formulation for the glacier length:

$$\frac{dL}{dt} = \frac{\dot{b} (w_0 L + w_1 \Lambda(L))}{\frac{\alpha_m}{1+\nu_s} L^{1/2} \left(\frac{5}{2} w_0 + \frac{3}{2} \frac{w_1}{L} \Lambda(L) + w_1 L e^{-w_2 L} \right)} \quad (6)$$

where $\Lambda(L) = w_2^{-2} (1 - w_2 L e^{-w_2 L} - e^{-w_2 L})$ is used to obtain an easy-to-read final equation. However, this formulation requires more data on the modeled glacier, which are not always available, and it adds more free parameters to our simple model.

Finally, in the following, B_s is obtained from direct mass balance measurements, and the glacier length variations estimated by the model are compared with data on glacier snout fluctuations. Since mass balance data are usually available on shorter time spans than snout fluctuation measurements, we need to extend the mass balance information. To this end, various methods can be used, ranging from simple empirical relation to complex energy balance models. Here, we have only series of temperature and precipitation values, which restrict the complexity of the method to be used. For this reason, we use an empirical relationship between mass balance and climatic variables such as June-September temperature and October-May precipitation, starting from the years when the mass balance is measured. Such an empirical relationship is then used to estimate the mass balance from climatic variables, for the years when direct balance data are not available and for future climatic conditions. A similar approach was used by Calmanti & alii (2007) to link glacier length fluctuations to climatic variability in previous years; here, we use a direct, same-year relationship between glacier mass balance and climate. This approximation is justified by the small size of the considered glaciers, which allow to assume a fast response to climate forcing. Other simple methods could be used to link surface mass balance to climate variable, such as the Positive Degree Day (PDD) method by Reeh (1991), which leads to similar surface mass balance reconstructions (not shown).

MODELING RESULTS

Ciardoney and Grand Etrèt glaciers

First of all, we considered the standardized temperature and precipitation time series that refer to the two boxes of ARPA's Optimal Interpolation grid in which the two glaciers are located. These two climatic variables have been related to the measured mass balance series using a bivariate fit:

$$\dot{b}_i = a T_{s,i} + b P_{w,i} + c \quad (7)$$

where \dot{b}_i represents the punctual mass loss or gain for the i th year, $T_{s,i}$ is the standardized June-September temperature and $P_{w,i}$ is the standardized October-May precipitation for the same year. These values are standardized using the method described before. The three parameters represent the influence of June-September temperature (a), October-May precipitation (b) and other factors affecting the mass balance (c), such as glacier shape, glacier exposition, topography, debris coverage, direct radiation, etc.

A fit between the measured mass balance and the climate data over the years in which the mass balance observations are available provides the parameters values reported in table 3. Note that the mass balance is measured in meters of water equivalent (*mve*) per year.

Now we use the mass balance reconstructed using Eq. (7) to force and integrate the two cases of minimal model Eq. (4) and Eq. (6). For the model with a fixed glacier width we set one parameter (ν) from literature (Oerlemans, 2011) and we tune parameter (α_m) in order to minimize the root mean square (RMS) difference between the measured glacier length variations and the modeled ones. For the case in which the glacier width varies along the flowline, we set two parameters (ν and w_1) to general values from literature (Oerlemans, 2011); the two parameters w_0 and w_2 are set according to geometrical information, which is available for these glaciers and α_m is tuned as described above. The parameter values used for the simulations are summarized in table 2.

Figures 5a, b show that over the full period over which length measurements are available we find a good match

TABLE 3 - Values of the parameters a , b and c used in the relation between mass balance and climatic variables for Ciardoney Glacier and Grand Etrèt Glacier. a represents the impact of June-September temperature, b the influence of October-May precipitation and c the impact of other factors on the mass balance. (Meas.) refers to values obtained directly using the measured mass balance, standard June-September temperature and standard October-May precipitation series. (Mod.) refers to values obtained with the minimization of the root mean squared difference, D , between the measured glacier length variations and the modeled ones. The rightmost column ($D_{\%}$) reports the value of D as relative difference with respect to the entire glacier length

Glacier	a	b	c	$D(a,b,c)$	$D_{\%}$
	[mwe year ⁻¹]	[mwe year ⁻¹]	[mwe year ⁻¹]	[m]	[%]
Ciardoney (meas.)	-0.48 ± 0.42	0.63 ± 0.49	-0.85 ± 0.43		
Ciardoney (mod.)	-0.44	0.75	-0.78	11.1	0.7
Grand Etrèt (meas.)	0.06 ± 0.32	0.67 ± 0.22	-0.97 ± 0.28		
Grand Etrèt (mod.)	-0.01	0.37	-0.98	4.1	0.3

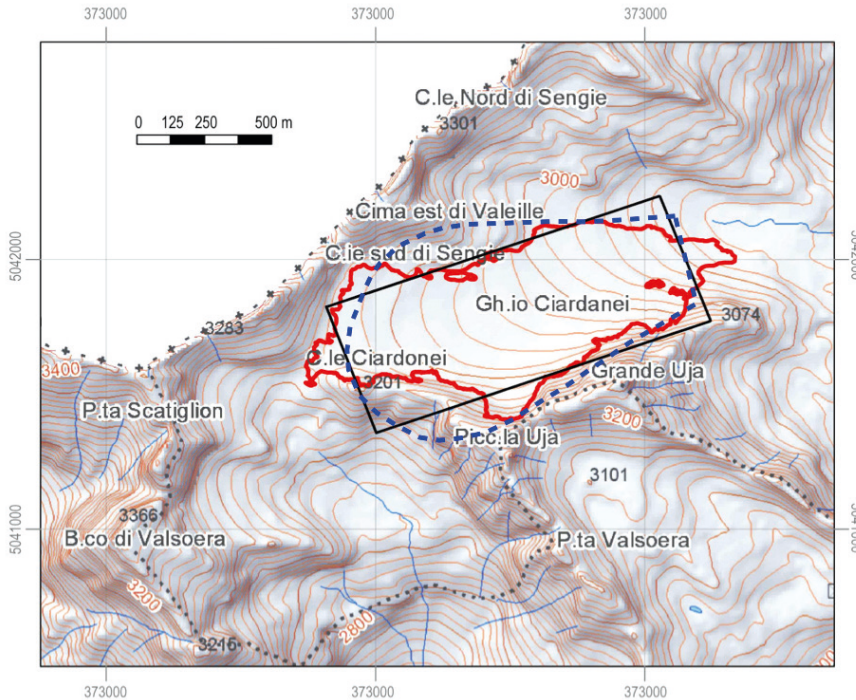


FIG. 4 - The Ciardoney Glacier and its representation in the minimal model. The glacier contour is outlined by the red line. The blackbox represents the simplified glacier geometry used in the basic case model while the blue dashed line gives the shape described in Eq. (5). Map based on the digital topographic map (1:50000) of the Regional Agency for Environmental Protection of Piedmont (ARPA Piemonte), 2011. Graphic by S.Lucchesi.

(difference smaller than 2.5% of the glacier length) between the lengths dynamics determined from the reconstructed mass balance (Eq. (7), red and blue continuous lines) and the observed length fluctuations (circles). Since the coefficients in Eq. (7) have been determined only in the period in which the mass balance measurements were available, we can consider the other years as an example of out-of-sample prediction. In the following, other glaciers, for which even less information are available (no mass balance measurements), will be studied using only the simpler model Eq. (4).

The green continuous lines in figures 5a,b represent the reconstructed glacier lengths when climate simulations from the EC-Earth model are used as forcing instead of the local OI measurements. Since these are climate simulations, in this case we cannot expect a year-by-year correspondence with the actual length variations. Furthermore, the EC-Earth fields present a lower resolution compared to the OI fields. Despite these issues, it is interesting to notice that the

main trends for both Ciardoney and Grand Etrèt glaciers are also captured, with differences smaller than 5% of the glacier length.

The sensitivity of our approach (mass balance estimate plus glacier model) has been tested for the case of a fixed glacier width, using two different methods. The first method considers the difference between the mass balance values obtained from Eq. (7) and the measured values as residuals due to a background noise. The standard deviation of this residual, σ_r , is introduced in Eq. (7) multiplied by a Gaussian white noise term, w_i :

$$\dot{b}_i = a T_{s,i} + b P_{w,i} + c + \sigma_r w_i \quad (8)$$

We compute 100 independent realizations of the integrated time series using independent random forcing and from these we determine a 90% confidence region for the model's results, shown as a light gray range in figures 5a, b.

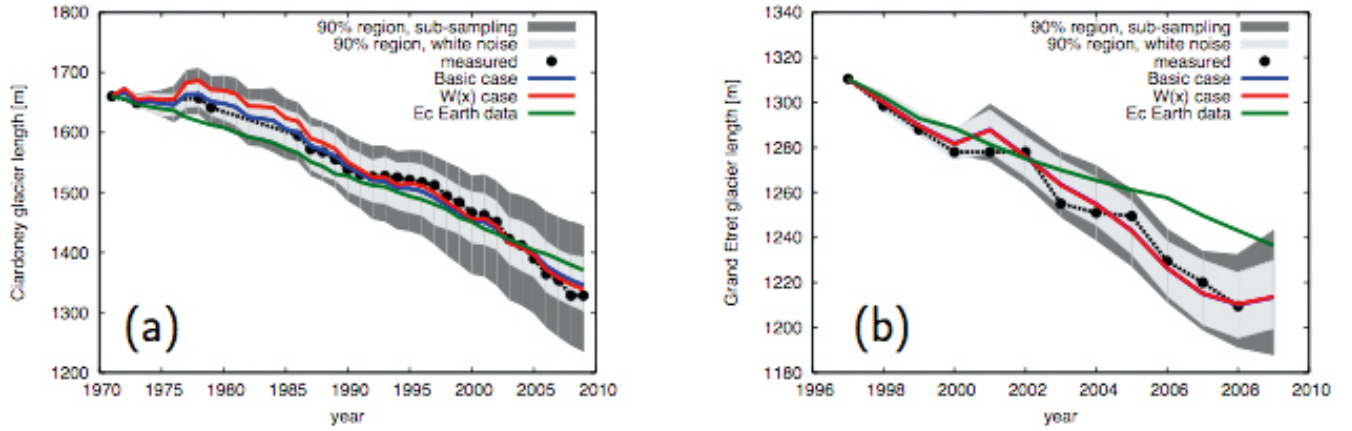


FIG. 5 - Application of the minimal model to the Ciardoney Glacier (a), and to the Grand Etrèt Glacier (b). Geometrical model parameters are in Tables 1 and 2. Equation (7) gives the relation between climate variations and surface mass balance values, while Eqs. (4) and (6) give the glacier dynamics. Circles indicate years with measured length variation while the straight blue line represents the model result obtained using the Basic case (Eq. (4)), while the straight red line represents the model result obtained using the $W(x)$ case (Eq. (6)). Finally the straight green line represents the basic case result forced with the ensemble mean of the EC-Earth model. The dark gray area is the 90% confidence region obtained with the “sub-sampling” method while the light gray area is obtained with the “white noise” method, both of them applied to the basic case.

The other method consists in sub-sampling the series of measured mass balance, standard precipitation and standard temperature obtaining subsamples with half the original length (18 values for the Ciardoney Glacier and 10 values for the Grand Etrèt Glacier), from which the sensitivity to the fit parameters can be evaluated. Here, 1000 series are created by sub-sampling the original one. The 90% confidence bands obtained with this method are shown in figures 5a,b with dark gray bands. This error analysis shows that the model is more sensitive to the fit parameters in Eq. (7) than to an internal noise.

The Ciardoney and the Grand Etrèt glaciers are only a few kilometers apart, but still present different local features, for example the two glaciers differ in their aspect (Ciardoney faces east, Grand Etrèt faces north-west). These local conditions lead to a different relation between mass balance and climatic parameters for the two glaciers, as also obtained in other Alpine areas (e.g. Kuhn, 1985). For example, the Grand Etrèt Glacier shows a stronger dependency of mass balance on precipitation rather than on temperature. This behavior challenges previous studies that assess that Alpine glaciers, at least in recent decades, are more sensitive to changes in temperature than precipitation (e.g. Thibert & *alii*, 2013; Steiner & *alii*, 2008). According to Steiner & *alii* (2008), sensitivity to precipitation rather than temperature is a characteristic of maritime glaciers in contrast to continental glaciers. Vincent & *alii* (2005) attribute the onset of the Little Ice Age (fifteenth to nineteenth centuries) retreat and subsequent periods of re-advances in the European Alps to changes in winter precipitation rather than on temperature. In general, the differences in the relation between mass balance and climate forcing obtained here highlight the importance to take into account the spatial and temporal diversity of mountain glaciers when analyzing their response to climate variations (Winkler & *alii*, 2010).

Glaciers without measured mass balance

The model presented in this work needs measured values of mass balance to attain a relation between mass balance and climatic fluctuations. Unfortunately, mass balance data are available only for a small number of glaciers, while measures of length variations have been collected for the last one hundred years for many of the Italian glaciers. Also considering that a general relation between mass balance and climatic factors cannot be easily found, as shown by the cases of the Ciardoney and Grand Etrèt glaciers, a simple empirical mass balance reconstruction is required.

Assuming that the mass balance is related to the climate variables with the same Eq. (7) used above, we seek the combination of a , b , c that minimizes the RMS difference between the measured glacier length variations and the modeled ones when the minimal model Eq. (4) is applied, after setting the value of α_m to a general value, here, $\alpha_m = 7 [m^{1/2}]$, since no specific information is available. In particular we minimize

$$D(a, b, c) = \sqrt{\frac{\sum(L-L_m)^2}{n}} \quad (9)$$

where L_m are the measured lengths and L are those obtained from the model. The sum is over the years present in both series, and n is the number of the common years. For the climate variables we use the standardized June-September temperature and October-May precipitation in the box of the ARPA's Optimal Interpolation grid that contains the glacier. This minimization is achieved by computing many different parameter combinations of a , b and c .

As an initial validation, this procedure has been applied to the Ciardoney and Grand Etrèt glaciers, for which a direct relation between mass balance and climatic variables has already been determined in the previous section.

TABLE 4 - Values of the three parameters for Eq. (7) used in the mass balance reconstruction, obtained with the minimization of the root mean squared difference, D , between the measured glacier length variations and the modeled ones. The rightmost column ($D_{\%}$) reports the value of D as relative difference with respect to the entire glacier length

Glacier	a	b	c	D(a,b,c)	D _%
	[mwe year ⁻¹]	[mwe year ⁻¹]	[mwe year ⁻¹]	[m]	[%]
Basei	-0.22	0.01	-0.06	3.5	0.5
Bessanese	-0.11	0.13	0.01	1.7	0.1
Capra	-0.28	0.18	-0.18	3.8	0.4
Lys	-0.39	0.90	0.01	31.0	0.6
Moncorvè	-0.14	-0.02	-0.15	5.7	0.4
Mulinet Nord	-0.03	-0.04	-0.10	1.6	0.4
Mulinet Sud	-0.06	-0.04	-0.25	2.8	0.4
Prè de Bar	-0.82	-1.32	0.16	76.6	2.3
Valtournanche	-0.06	0.08	-0.17	4.1	0.3

Table 3 compares the best parameter values for Ciardoney and Grand Ètrèt obtained using the direct method and the minimization method. The parameters values of the Ciardoney Glacier displayed in table 3 are similar in the two cases, while the parameters values of the Grand Ètrèt Glacier show a similar behavior except for b , which displays a larger influence on the mass balance in the measured case compared to the modeled one.

We applied the method to nine glaciers of the northwestern Italian Alps without an observed mass balance, namely Basei, Bessanese, Capra, Lys, Moncorvè, Mulinet Nord, Mulinet Sud, Prè de Bar and Valtournanche (see fig. 1). The geometry information required by the model for these glaciers is described in table 1. The parameter values resulting from the minimization procedure are listed in table 4. Note that, only for the Prè de Bar glacier, we obtain a RMS with values larger than 1% of the glacier length ($D_{\%}$ in table 4). Figure 6 reports the corresponding evolution of glacier lengths obtained from the model Eq. (4). In order to gauge the sensitivity to the parameter estimates in table 4, we repeated the minimization process sampling randomly subsets of years formed by half of the available years. We repeated this process 100 times, to obtain 90% confidence regions, which are reported as light-gray shaded areas in the figure 6.

Each of the glaciers considered here has different characteristics, such as shape, aspect, volume, etc., which can influence the accuracy of the obtained results (see Appendix A). The accuracy of the results can be represented using the RMS difference between the measured series of length variations and the modeled one obtained using the parameter values in tables 3 and 4. These tables highlight that our model works better with small glaciers, with a length ranging from few hundreds of meters to about 2000 m, while the RMS difference is very large for the two largest glaciers, the Prè de Bar and Lys glaciers. In particular, the Prè de Bar Glacier exhibits the highest value of the RMS difference reaching a difference of about 2.3% of the glacier length (table 4).

The glaciers considered in this work, in general, show a significant retreat in the last decades, which has also been observed in other Alpine regions (e.g. Paul & alii, 2004;

Diolaiuti & alii, 2012). If we analyze in detail the model results, the nine glaciers can be divided into three groups, which we discuss more in detail in the following.

Basei, Bessanese, and Capra glaciers

These three glaciers show a good agreement between measured and modeled values (fig. 6a-c). The main feature for Basei, Bessanese, and Capra glaciers is the presence of a gap in the observation during the two decades from 1970 to 1990. In those years, a short re-advance period is documented for the Alpine glaciers (Zemp & alii, 2006, 2008), and the model reproduces this increase in glacier length. This reconstruction supports the presented method since it adds information on the glacier evolution during the period in which these glaciers were not surveyed.

Lys and Prè de Bar glaciers

These two glaciers present a measured line much smoother than the modeled one (fig. 6d and h). This discrepancy can be attributed to the difference between the instantaneous response time assumed by the model and the actual finite response of glacier length, which is delayed, filtered and conditioned by glacier dynamics (Thibert & alii, 2013).

Moreover, these two glaciers, also because of their extension, have a complex setting and geometry: they are both characterized by a well-defined tongue, which connects to the accumulation area through a marked rock step. The tongue of the Lys Glacier, in addition, is fed by two separate accumulation basins.

In this case, the absence of measured mass balance series creates a lack of knowledge that cannot be compensated with the empirical method presented.

Moncorvè, Mulinet Nord, Mulinet Sud, and Valtournanche glaciers

In the case of these glaciers, the model reproduces well the measured length oscillations (fig. 6e-g and i). It has to be pointed out that these glaciers show a predominance of the

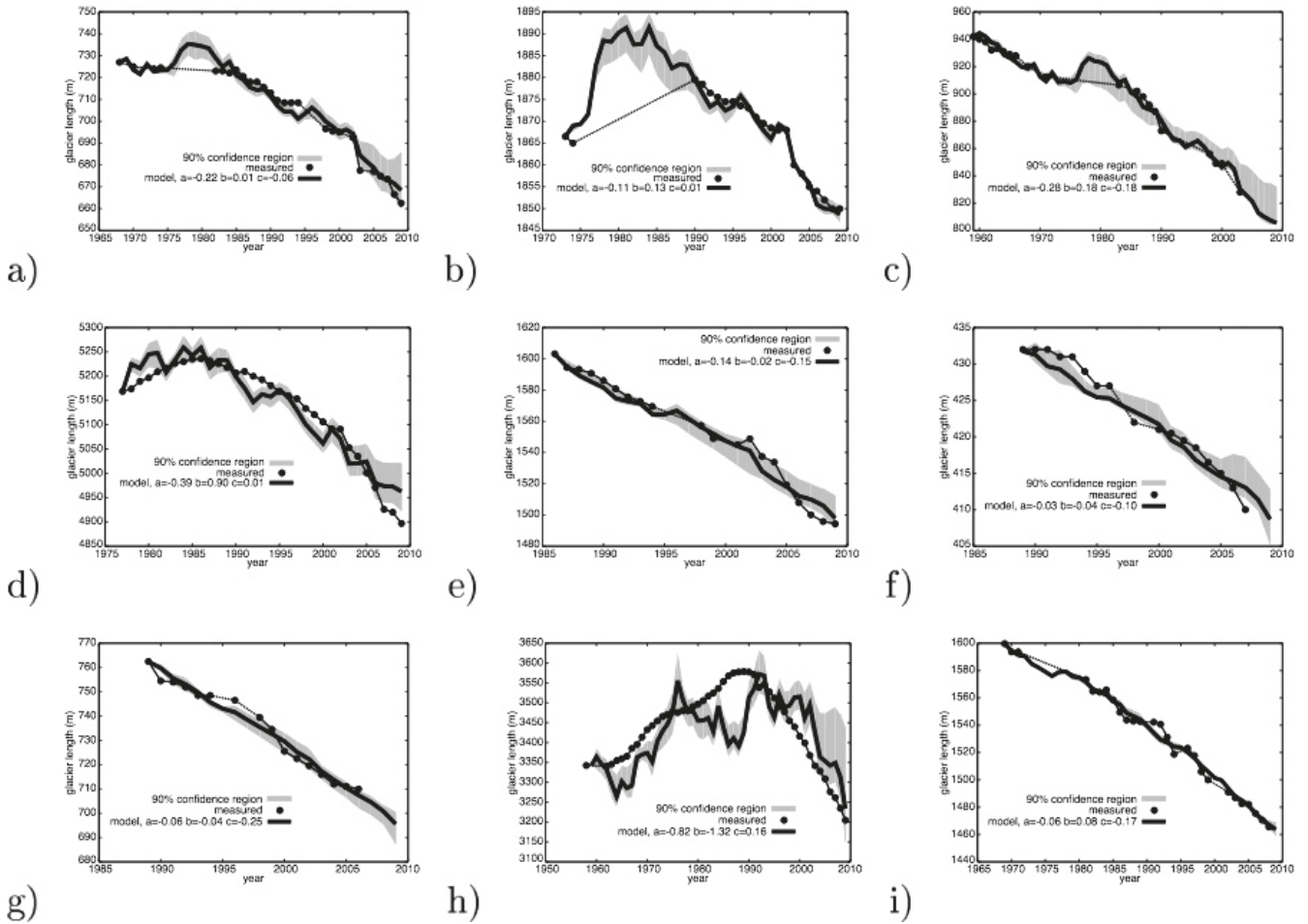


FIG. 6 - Application of the model using the values of Table 4. The circles indicate years with measured data and the thick black line is the model result. The shaded area represents the 90% confidence region obtained using 100 cases of sub-sampled series of measured length variations. (a) Basei glacier; (b) Bessanese glacier; (c) Capra glacier; (d) Lys glacier; (e) Moncorvè glacier; (f) Mulinet Nord glacier; (g) Mulinet Sud glacier; (h) Prè de Bar glacier; (i) Valtournanche glacier.

third term (c), see table 4, which represents the influence of external forcing different from October-May precipitation and June-September temperature changes, such as glacier shape, glacier exposition, topography, debris coverage, direct radiation, etc. This strong dependence on the last parameter explains the almost linear shape of the modeled length variations of these four glaciers. Consequently, only more complex model can give a complete description of the evolution of this set of glaciers, which are mainly influenced by these “non-climatic” features.

Future projections

One possible application of mathematical models is to estimate future glacier evolution. This can be done with the aid of future climate scenario projections from global climate models. In this work we use an ensemble of RCP 4.5 and RCP 8.5 scenarios produced with the global model EC-Earth for the CMIP5.

Figure 7 shows the future evolution of temperature and precipitation, for the seven monthly ensemble members for

RCP 4.5 and the eight monthly ensemble members for RCP 8.5, in the pixel of the EC-Earth model grid containing most of the glaciers. Figure 7a shows no great difference in precipitation in the two considered scenarios, but fig. 7b shows a considerable difference in the temperature evolution, with the temperatures increasing significantly more in the RCP 8.5 scenario compared to the RCP 4.5 scenario.

Using these climate projections, we estimate the future evolution of each glacier analyzed in the previous section using the dynamical model for length (Eq. 4) and the same parameters for Eq. (7) found in the historical period. These future projections are performed keeping in mind the limitations of our method, such as using a “box” shape for the glacier, considering an immediate response of the glacier to climate forcing, and assuming a constant value in time for the model parameters (a , b , c , α_{m} and v). Furthermore, we should keep in mind the model limits in simulating the glacier length for six glaciers out of eleven, namely Lys, Prè de Bar, Moncorvè, Mulinet Nord, Mulinet Sud, and Valtournanche glaciers. In fact, the minimal model is able to

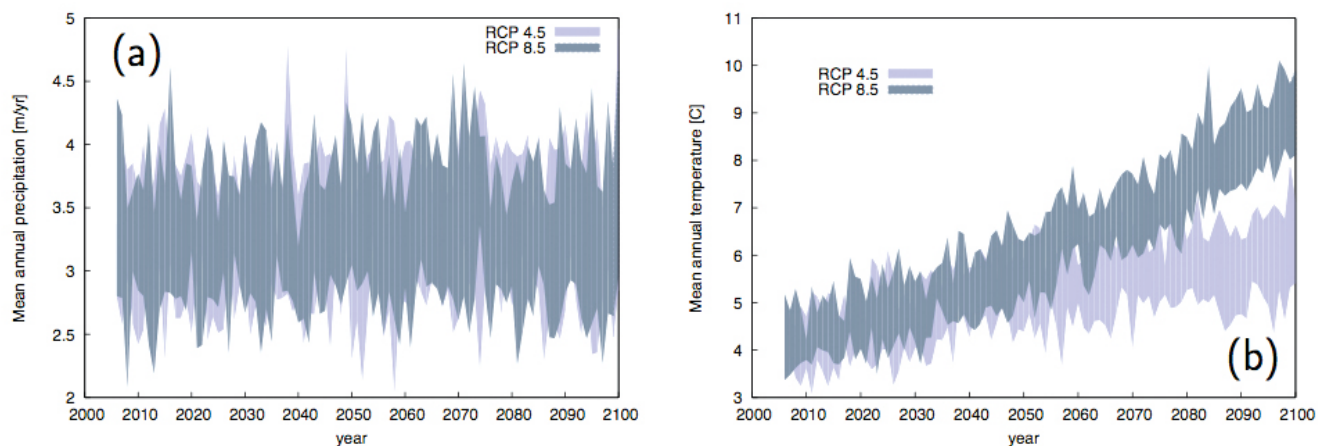


FIG. 7 - (a) Precipitation and (b) temperature variations estimated from an ensemble of EC-Earth realizations in the RCP 4.5 (7 monthly cases) and RCP 8.5 (8 monthly cases) future scenarios, for the GCM grid point containing most of the considered glaciers.

reconstruct the general trend of these glaciers and not their interannual variability, as described before. For each glacier we force the model with temperature and precipitation series ranging from 1959 to 2100 for the corresponding pixel of the EC Earth model grid.

The annual series of mean temperature and total precipitation are standardized using 1971-2000 as a reference period. Subsequently, the mass balance series are obtained using Eq. (7), with the parameters values reported in tables 3 and 4. Finally the minimal model Eq. (4) can be applied, using the geometry information in table 1. Figure 8 shows the future evolution of the eleven studied glaciers. The gray bands indicate the range in lengths covered by the ensemble members.

In general, the eleven glaciers exhibit a decrease in their length characterized by a severe shrinkage by the end of the 21st century, which is in line with the simulated variations by previous works (e.g. Zemp & *alii*, 2006; Salzmann & *alii*, 2012; Linsbauer & *alii*, 2013). The RCP 8.5 scenario presents a larger glacier retreat with respect to RCP 4.5 scenario due to its higher predicted increase in temperature (fig. 7b). Each glacier shows a different behavior according to the different influence of the two climatic variables on the mass balance relation (see tables 3 and 4). In general, glaciers with a stronger influence of the third term, c , present a smaller ensemble spread, while glaciers with large values of a and b show a larger ensemble spread and a larger difference between the two scenarios.

The Prè de Bar Glacier is the only glacier predicted to disappear before the year 2100 (fig. 8j). The RCP 4.5 scenario forecasts the glacier disappearance in the period 2080-2100, while RCP 8.5 scenario in the period 2070-2080. It is important to recall that the Prè de Bar Glacier behavior, due to its dimensions and others features, is not very well described by the simple model used in this work, so that this prediction should be considered with caution. Anyhow, more complex models show also a retreating behavior for Alpine glaciers during the 21st century, and even large glaciers have been predicted to have a strong

shrinkage during this century (e.g. LeMeur & *alii*, 2007; Jouvè & *alii*, 2011).

The model results indicate that the eleven glaciers considered here are going to decrease in length during this century and that the rate of retreat depends strongly on the future scenario which is used. Some mechanisms, which are not considered in this work, such as change in debris cover, glacier surge or breaking apart of part of the glacier, could change the glacier retreating behavior. Nevertheless, the model results presented here can give, at least, an order of magnitude estimation of glaciers retreat during this century.

DISCUSSION AND CONCLUSION

The application of the minimal model illustrated in this paper to a sample of glaciers in the Western Italian Alps confirms that modeling glacier dynamics is a complex task. In fact, the considered glaciers show very different behaviors in response to climate forcing. This outcome can be partly explained with the different dimension of the studied glaciers, whose surface ranges from 0.2 to over 9 km²: in fact the largest discrepancies are obtained for the largest glaciers (Lys and Prè de Bar). These limitations could be linked to the simplicity of the model, which considers a “box” shape that is too rough for glaciers with complex geometry such as Lys and Prè de Bar. Furthermore, large glaciers show a delayed and long-term response to climate forcing, which should be taken into account. This effect is particularly relevant when mass balance data are not available and glacier dynamics has to be inferred only from changes of glacier length.

The smaller glaciers show different behaviors with respect to climatic parameters: some of them (Capra, Basei) appear to be mainly influenced by June-September temperature, while others are more sensitive to October-May precipitation (Bessanese, Grand Etrèt): this unexpected behavior has been observed also in other regions of the Alps (Vincent & *alii*, 2005).

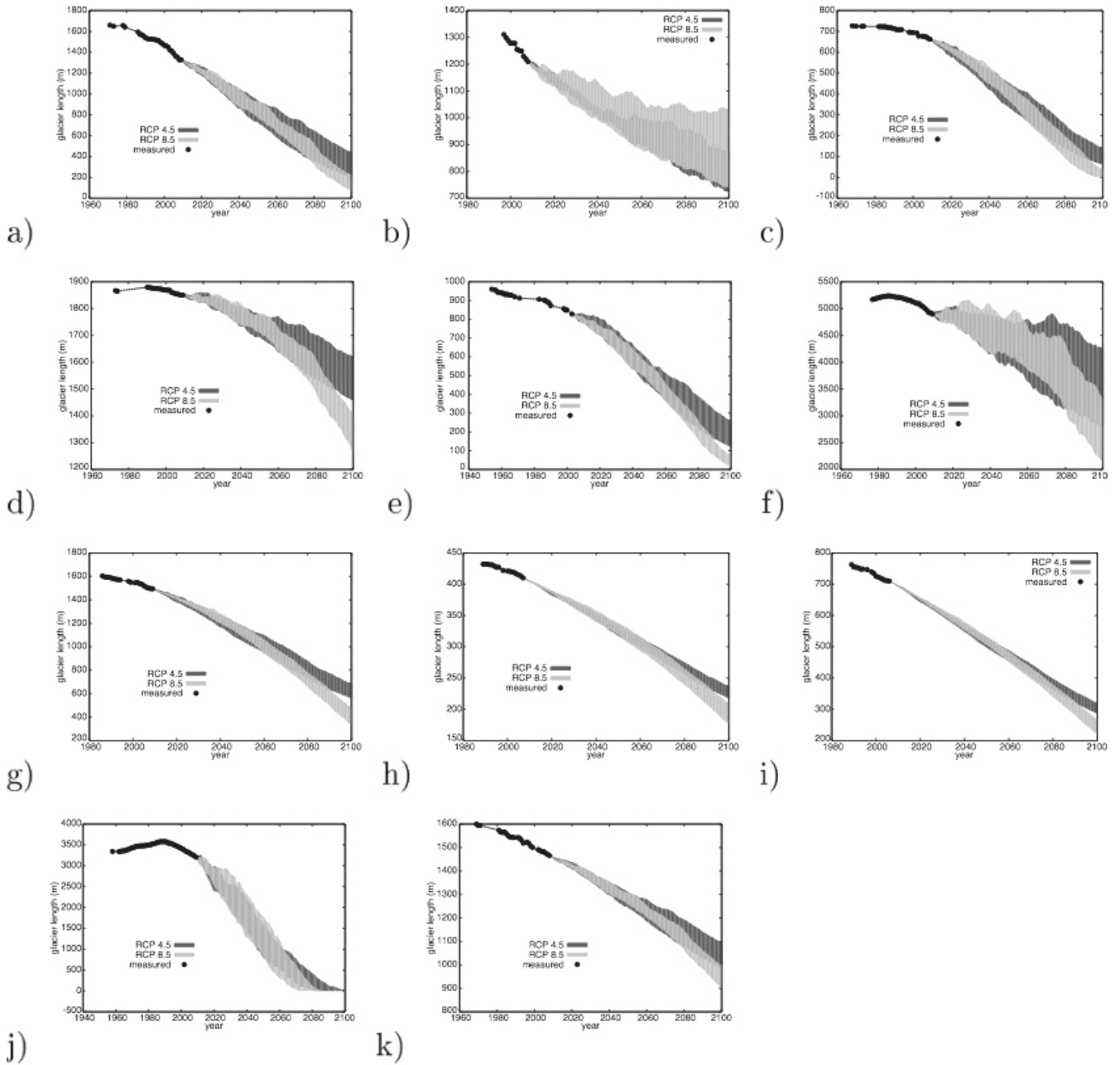


FIG. 8 - Future evolution of glacier lengths obtained using an ensemble of EC-Earth simulations in the future scenario RCP 4.5, and in the future scenario RCP 8.5. Circles represent the measured values of glacier length in the historical period. (a) Ciardoney glacier; (b) Grand Etrèt Glacier; (c) Basei Glacier; (d) Bessanese Glacier; (e) Capra Glacier; (f) Lys Glacier; (g) Moncorvè Glacier; (h) Mulinet Nord Glacier; (i) Mulinet Sud Glacier; (j) Prè de Bar Glacier; (k) Valtournanche Glacier. The gray bands indicate the spread in lengths obtained from the different ensemble members. Notice that the spreads of the two scenarios should not be compared directly since they are based on a different number of ensemble members.

Finally, for a third group of glaciers, additional factors other than climatic parameters appear to play an important role (Moncorvè, Mulinet Nord, Mulinet Sud, and Valtournanche). While more complex models may be better suited to model the response of such glaciers, the absence of some information, starting from the ice thickness profile along the flow line, limit the complexity of the applicable models. For example, the high order flow

line model presented by Pattyn (2002) cannot be used here. In these cases the varying ice thickness profile could be only estimated using a general theoretical profile, e.g. using the A-V method presented by Harrison (2013) or the method by Huss & Farinotti (2012).

When we consider future projections, the first group of glaciers, which is influenced mainly by temperature in the historical period, shows a higher retreat in length, i.e. both

Capra and Basei reach zero length around 2100 in the RCP 8.5 scenario (fig. 8c, e). The other glaciers show a slower retreat (see for example the Grand Etrèt Glacier, fig. 8b).

Among the eleven glaciers which we considered, the Ciardoney Glacier presents the longest series of measured mass balances, and also a complete series of measured frontal length variations: this wealth of data makes the Ciardoney Glacier the most reliable study case for testing past reconstruction and future prediction of glacier change in response to climate variability.

In general, the shortage of information on the studied glacier increases the uncertainties of our approach. In particular the relation between meteorological data and mass balance (Eq. (7)) represents the largest uncertain point of our model. We tested the sensitivity of our approach to the estimate of the three parameters a , b , and c by using a sub-sampling method. The uncertainties obtained with this method exhibit a larger influence on the final glacier length reconstruction with respect to the uncertainties created by an internal noise.

Furthermore, also the lack of knowledge on the ice thickness influences the uncertainties in our model. In fact, the parameters α_m and ν in Eq. (1) are set to general values for the nine glaciers without measured mass balances, due to the absence of this specific information.

Glacier volume, form, altitude, debris coverage, and aspect can significantly contribute to determine glacier dynamics in response to climate forcing. However, the contribution of each of these factors is difficult to estimate and no univocal contribution can be extracted from published literature. These features could be taken into account in more complex model, especially, when applied to glaciers where these characteristics have been measured and studied. In particular the applicability of the model to evaluate future projections is constrained by these factors. We assume a constant value in time for the model parameters but we don't have any information on how the climate features will influence the glacier surface mass balance in future. This assumption, then, limits the length and the reliability of our future simulations.

Despite all the above mentioned limitations, the minimal model presented here has been shown to be a useful tool for a rapid, preliminary assessment of the sensitivity of small glaciers (which are the majority of glaciers in the Italian Alps, see Salvatore & alii, 2015) to regionalized climatic parameters and it allows to simulate the evolution of these glaciers in response to different future climate scenarios.

APPENDIX A: CHARACTERISTICS OF THE GLACIERS CONSIDERED IN THIS STUDY

A.1 Ciardoney

The Ciardoney Glacier lies on the southern flank of the Gran Paradiso massif, in a cirque located at the head of the Forzo Valley. It has a surface of only 0.58 km², but it ranks third among the Glaciers of the Orco and Soana valleys. Its morphological characteristics (low surface gradient

and limited crevassing) make the Ciardoney Glacier very suitable for glaciological measures. Starting in 1992, it has thus become the object of a series of mass balance measurements that now has few equals in the Italian Alps, for its length and completeness (Mercalli & Cat Berro, 2005). In addition, the glacier, whose elevation presently ranges from 3140 to 2850 *m a.s.l.*, has a quite regular shape, with a present length of 1350 *m* and a maximum width of 580 *m*, and a uniform aspect, and is thus also suitable for our modeling purposes (fig. 4).

A.2 Grand Etrèt

The glacier occupies the head of the Valsavaranche Valley, on the northern flank of the Gran Paradiso massif, and has a prevalent aspect to the North. Since 1999, it has been chosen for mass balance measures, as representative of glaciers behavior on the northern side of the Gran Paradiso National Park (Bertoglio & Cerise, 2008). In fact, it has a fairly small area (0.56 km²), together with a low gradient and smooth surface. Due to the enhanced shrinkage occurred in the last decades, the current shape of the glacier is quite regular and therefore suitable for the geometry simplification required by the model. According to the glacier inventory ("Catasto Ghiacciai") of the Valle d'Aosta Region, the glacier ranges in elevation from 3100 to 2700 *m a.s.l.*; in 1999, its maximum length was 1.35 km, and its maximum width was 0.87 km. A Ground Penetrating Radar (GPR) survey performed in 2006 showed that the glacier reaches a thickness of 43 *m* in its central portion. This information can be used to determine the basal shear stress of the glacier through a relation between ice thickness

$$(H), \text{ slope } \left(\left| \frac{dh}{dx} \right| \right) \text{ and shear stress. } (\tau_0): \rho g H \left| \frac{dh}{dx} \right| = \tau_0.$$

Consequently, a shape for the ice thickness along the flowline might be determined. However, this method applies only to the Grand Etrèt Glacier and cannot be used as a general method, which is the aim of this work.

A.3 Basei

The glacier covers the northeastern flank of the Basei Peak (Gran Paradiso massif), from an elevation of 3300 *m* to 2950 *m a.s.l.* The current (2006) area is about 0.26 km², while the maximum length and width are respectively 0.85 and 0.50 km. Thanks to the lack of high rock walls around the glacier, its surface is free of debris, at variance to most other glaciers that are also experiencing a prolonged phase of retreat. Due to its location in a glacial depression, changes in length in response to climatic factors are less marked than for other glaciers (e.g. Ciardoney Glacier).

A.4 Bessanese

In the Valle Grande di Lanzo, the Bessanese Peak dominates the large cirque hosting the glacier, whose maximum altitude is 3220 *m a.s.l.* The glacier has a well-developed tongue (a smaller one, on the left side of the

glacier, is now extinct), which flows down to an elevation of 2580 *m a.s.l.* and is now masked by a thick debris cover, as a result of the marked retreat of the last decades. The overall area, facing S-SE, was 0.50 km² in 2006, with a maximum length of almost 2 km and a maximum width of about 0.7 km.

A.5 Capra

Thanks also to its N-NE exposition, this glacier has the lowest front elevation (2450 *m a.s.l.*) of the entire Gran Paradiso massif, while its maximum altitude is 2800 *m a.s.l.* The glacier (0.25 km²) is composed of an accumulation area located in a well-defined cirque, and of the remains of a tongue, which during the Little Ice Age has built impressive lateral moraines and is now completely covered with debris. Total glacier length is about 0.9 km, and its maximum width is 0.5 km.

A.6 Lys

It is the largest glacier considered in this study (9.59 km² in 2005). It is located on the southern flank of the Monte Rosa massif and it is enclosed to the North by the Eastern Liskamm crest. It is formed by a compound accumulation area reaching a maximum elevation of 4350 *m a.s.l.*, feeding two distinct branches which join at an elevation of about 2700 *m* to form a single, large tongue (named "Plateau"), flowing down to an altitude of 2355 *m*. Maximum length and width, measured in 1999, were respectively 5.2 km and 5.6 km.

A.7 Moncorvè

The main glacial body is currently resting along the northern side of the Ciarforón Peak (Gran Paradiso), with a smaller body on the western flank of the Tresenta Peak, which is on the point of detaching from the main one to the east. The glacier has an area of about 1.3 km² and is more developed in width than in length (1.5 km and 2.0 km respectively, measured in 1999). Glacier elevation ranges from 3640 *m* to about 2900 *m*, with the front plunging in a large moraine lake.

A.8 Mulinet Nord and Mulinet Sud

These two glaciers occupy two adjoining topographic depressions in a large cirque between the Monfret and Martellot peaks (Valle Grande di Lanzo). They used to be a unique glacier at the beginning of the 20th century, but the subsequent phase of glacier retreat led to the separation of the Mulinet Glacier in two bodies of similar surface (0.2 km² and 0.3 km², respectively, in 2006). After the marked retreat of the last decades, the glaciers have now a quite regular, almost rounded shape. The maximum elevation reached by the glaciers is about 3000 *m*, while the front is now located at about 2700 *m*, after that in 2007 the small tongues detached from the accumulation areas, in correspondence of the rock step which borders the glacial cirque towards valley.

A.9 Prè de Bar

Located at the very end of the Ferret Valley (Mont Blanc), this glacier has a surface of about 3 km². It is one of the most famous glaciers of the Aosta Valley, because of its distinctive lobated tongue, easily accessible from the main valley bottom. In the last few years, though, the morphology of the glacier front has changed dramatically, with a marked regression of the glacial tongue (at an approximate elevation of 2090 *m a.s.l.*), which during the summer 2012 finally detached from the accumulation basin, in correspondence of a marked rock step. Glacier maximum length and width were respectively 3.3 km and 2.7 km in 1999.

A.10 Valtournanche

It is a glacier of about 1 km², which flows west from the ridge between the Testa Grigia Peak (3480 *m a.s.l.*) and the Gobba di Rollin, in Valtournanche (Monte Rosa group). The glacier front is now at an elevation of about 3000 *m*.

REFERENCES

- BENISTON M. (2012) - *Impacts of climatic change on water and associated economic activities in the Swiss Alps*. Journal of Hydrology, 412-413, 291-296.
- BERTOGGIO V. & CERISE S. (2008) - *Evoluzione del ghiacciaio del Grand Etret*, in: Environnement, 41, Regione Autonoma Valle d'Aosta, available at: <https://www.regione.vda.it/gestione/riviweb/templates/aspx/environnement.aspx?pkArt=383> (last access: July 2012).
- BONANNO R., RONCHI C., CAGNAZZI B. & PROVENZALE A. (2013) - *Glacier response to current climate change and future scenarios in the northwestern Italian Alps*. Regional Environmental Change, 13, 1-11.
- BRAUN L.N., WEBER M. & SCHULZ M. (2000) - *Consequences of climate change for runoff from Alpine regions*. Annals of Glaciology, 31, 19-25.
- BRUNETTI M., MAUGERI M., MONTI F. & NANNI T. (2006) - *Temperature and precipitation variability in Italy in the last two centuries from homogenized instrumental time series*. International Journal of Climatology, 26, 345-381.
- CALMANTI S., MOTTA L., TURCO M. & PROVENZALE A. (2007) - *Impact of climate variability on Alpine glaciers in northwestern Italy*. International Journal of Climatology, 27, 2041-2053.
- CHIARLE M. & MORTARA G. (2008) - *Geomorphological impact of climate change on Alpine glacial and periglacial areas. Examples of processes and description of research needs*, in: Interpraevent 2008 -- Conference Proceedings, Dornbirn, 26-30 May 2008, 111-122.
- DELINÉ P., GARDENT M., MAGNIN F. & RAVANEL L. (2012) - *The morphodynamics of the Mont Blanc massif in a changing cryosphere: a comprehensive review*. Geografiska Annaler: Series A, Physical Geography, 94, 265-283.
- DIOLAIUTI G.A., BOCCHIOLA D., VAGLIASINDI M., D'AGATA C. & SMIRAGLIA C. (2012) - *The 1975-2005 glacier changes in Aosta Valley (Italy) and the relations with climate evolution*. Progress in Physical Geography, 36, 764-785.
- HARRISON W.D. (2013) - *How do glaciers respond to climate? Perspectives from the simplest models*. Journal of Glaciology, 59, 949-960.

- HAZELEGER W., WANG X., SEVERIJNS C., ȘTEFĂNESCU S., BINTANJA R., STERL A., WYSER K., SEMMLER T., YANG S., VAN DEN HURK B., VAN NOIJE T., VAN DER LINDEN E. & VAN DER WIEL K. (2012) - *EC-Earth V2.2: description and validation of a new seamless earth system prediction model*. *Climate Dynamics*, 39, 2611-2629.
- HUSS M. & FARINOTTI D. (2012) - *Distributed ice thickness and volume of all glaciers around the globe*. *Journal of Geophysical Research*, 117, F04010, doi:10.1029/2012JF002523.
- JOUVET G., HUSS M., FUNK M. & BLATTER H. (2011) - *Modelling the retreat of Grosser Aletschgletscher, Switzerland, in a changing climate*. *Journal of Glaciology*, 57, 1033-1045.
- KUHN M. (1985) *Fluctuations of climate and mass balance: different responses of two adjacent glaciers*. *Z. Gletscherkd Glazialgeol.*, 21, 409-416.
- LE MEUR E., GERBAUX M., SCHÄFER M. & VINCENT C. (2007) - *Disappearance of an Alpine glacier over the 21st century simulated from modeling its future surface mass balance*. *Earth and Planetary Science Letters*, 261, 367-374.
- LETRÉGUILLY A. (1988) - *Relation between the mass balance of western Canadian mountain glaciers and meteorological data*. *Journal of Glaciology*, 34, 11-18.
- LINSBAUER A., PAUL F., MACGUTH H. & HAEBERLI W. (2013) - *Comparing three different methods to model scenarios of future glacier change in the Swiss Alps*. *Annals of Glaciology*, 54, 241-253.
- MARZEION B., JAROSCH A.H. & HOFER M. (2012) - *Past and future sea-level change from the surface mass balance of glaciers*. *The Cryosphere*, 6, 1295-1322.
- MEIER M.F., DYURGEROV M.B., RICK U. K., O'NEEL S., PFEFFER W.T., ANDERSON R.S., ANDERSON S.P. & GLAZOVSKAYA. F. (2007) - *Glaciers dominate eustatic sea-level rise in the 21st century*. *Science*, 317, 1064, doi:10.1126/science.1143906.
- MERCALLI L. & CAT BERRO D. (2005) - *Clima acque e ghiacciai tra Gran Paradiso e Canavese*. 1st Edition, Società Meteorologica Subalpina, Bussoleno (TO), Italy.
- MOSS R.H., EDMONDS J.A., HIBBARD K.A., MANNING M.R., ROSE S.K., VAN VUUREN D.P., CARTER T.R., EMORI S., KAINUMA M., KRAM T., MEEHL G.A., MITCHELL J.F.B., NAKICENOVIC N., RIAHI K., SMITH S. J., STOUFFER R.J., THOMSON A.M., WEYANT J.P. & WILBANKS T.J. (2010) - *The next generation of scenarios for climate change research and assessment*. *Nature*, 463, 747-756, doi:10.1038/nature08823.
- NESSJE A. & DAHL S.O. (2000) - *Glaciers and Environmental Change*. 1st edition, Arnold, London, England.
- OERLEMANS J. (1997) - *A flowline model for Nigardsbreen, Norway: projection of future glacier length based on dynamic calibration with the historic record*. *Journal of Glaciology*, 24, 382-389.
- OERLEMANS J. (2001) - *Glaciers and Climate Change*. 1st edition, A.A. Balkema Publisher, Rotterdam, the Netherlands.
- OERLEMANS J. (2010) - *The Microclimate of Valley Glaciers*. Igitur, 1st print edition, Utrecht Publishing & Archiving Services, Universiteitsbibliotheek Utrecht, the Netherlands, 2010.
- OERLEMANS J. (2011) - *Minimal Glacier Models*. Igitur, 2nd print edition, Utrecht Publishing & Archiving Services, Universiteitsbibliotheek Utrecht, the Netherlands.
- OERLEMANS J., JANIA J. & KOLONDRAL L. (2011) - *Application of a minimal glacier model to Hansbreen, Svalbard*. *The Cryosphere*, 5, 1-11, doi:10.5194/tc-5-1-2011.
- PATTYN F. (2002) - *Transient glacier response with a higher-order numerical ice-flow model*. *Journal of Glaciology*, 48, 467-477.
- PAUL F., KÄÄB A., MAISCH M., KELLENBERGER T. & HAEBERLI W. (2004) - *Rapid disintegration of Alpine glaciers observed with satellite data*. *Geophysical Research Letters*, 31, L21402, doi:10.1029/2004GL020816.
- RAPER S.C.B. & BRAITHWAITE R. J. (2006) - *Low sea level rise projections from mountain glaciers icecaps under global warming*. *Nature*, 439, 311-313.
- REEH N. (1991) - *Parameterization of Melt Rate and Surface Temperature on the Greenland Ice Sheet*. *Polarforschung*, 5913, 113-128.
- SALZMANN N., MACHGUTH H. & LINSBAUER A. (2012) - *The Swiss Alpine glaciers' response to the global "2°C air temperature target"*. *Environmental Research Letters*, 7, 044001, doi:10.1088/1748-9326/7/4/044001.
- SALVATORE M.C., ZANONER T., BARONI C., CARTON A., BANCHIERI F., VIANIC., GIARDINO M. & PEROTTI L. (2015) - *The state of Italian glaciers: a snapshot of 2006-2007 hydrological period*. *Geografia Fisica e Dinamica Quaternaria*, 38 (2), 175-198.
- SMIRAGLIA C., AZZONI R.S., D'AGATA C., MARAGNO D., FUGAZZA D. & DIOLAIUTI G.A. (2015) - *The evolution of the Italian glaciers from the previous data base to the new Italian inventory. Preliminary considerations and results*. *Geografia Fisica e Dinamica Quaternaria*, 38 (1), 79-87.
- STEINER D., PAULING A., NUSSBAUMER S.U., NESJE A., LUTERBACHER J., WANNER H. & ZUMBÜHL H.J. (2008) - *Sensitivity of European glaciers to precipitation and temperature - two case studies*. *Climatic Change*, 90, 413-441.
- STOFFEL M. & HUGGEL C. (2012) - *Effects of climate change on mass movements in mountain environments*. *Progress in Physical Geography*, 36, 421-439.
- THIBERT E., ECKERT N. & VINCENT C. (2013) - *Climatic drivers of seasonal glacier mass balances: an analysis of 6 decades at Glacier de Sarennes (French Alps)*. *The Cryosphere*, 7, 47-66, doi:10.5194/tc-7-47-2013.
- UBOLDI F., LUSSANA C. & SALVATI M. (2008) - *Three-dimensional spatial interpolation of surface meteorological observations from high-resolution local networks*. *Meteorological Applications*, 15, 331-345.
- VINCENT C., LE MEUR E., SIX D. & FUNK M. (2005) - *Solving the paradox of the end of the Little Ice Age in the Alps*. *Geophysical Research Letters*, 32, L09706, doi:10.1029/2005GL022552.
- VIVIROLI D., ARCHER D.R., BUYTAERT W., FOWLER H.J., GREENWOOD G.B., HAMLET A.F., HUANG Y., KOBOLTSCHNIG G., LITAOR M.I., LÓPEZ-MORENO J.I., LORENTZ S., SCHÄDLER B., SCHREIER H., SCHWAIGER K., VUILLE M. & WOODS R. (2011) - *Climate change and mountain water resources: overview and recommendations for research, management and policy*. *Hydrological and Earth System Sciences*, 15, 471-504, doi:10.5194/hess-15-471-2011.
- WINKLER S., CHINN T., GÄRTNER-ROER I., NUSSBAUMER S.U., ZEMP M. & ZUMBÜHL H.J. (2010) - *An introduction to mountain glaciers as climate indicators with spatial and temporal diversity*. *ERDKUNDE*, 64, 97-118, doi:10.3112/erdkunde.2010.02.01.
- ZEMP M., HAEBERLI W., HOELZLE M. & PAUL F. (2006) - *Alpine glaciers to disappear within decades?* *Geophysical Research Letters*, 33, L13504, doi:10.1029/2006GL026319.
- ZEMP M., PAUL F., HOELZLE M. & HAEBERLI W. (2008) - *Glacier fluctuations in the European Alps 1850-2000: an overview and spatio-temporal analysis of available data*, in: *The Darkening Peaks: Glacial Retreat in Scientific and Social Context*, edited by: Orlove B., Wiegandt E. & Luckman B., University of California Press, Berkeley, 152-167.
- ZWINGER T., GREVE R., GAGLIARDINI O., SHIRAIWA T. & LYL Y. M. (2007) - *A full Stokes-flow thermo-mechanical model for firn and ice applied to the Gorskov crater glacier, Kamchatka*. *Annals of Glaciology*, 45, 29-37.

(Ms received 30 June 2015; accepted 15 February 2016)



Edizioni ETS
Piazza Carrara, 16-19, I-56126 Pisa
info@edizioniets.com - www.edizioniets.com
Finito di stampare nel mese di ottobre 2016